

RESEARCH

Open Access



Construction and optimization of a biocatalytic route for the synthesis of neomenthylamine from menthone

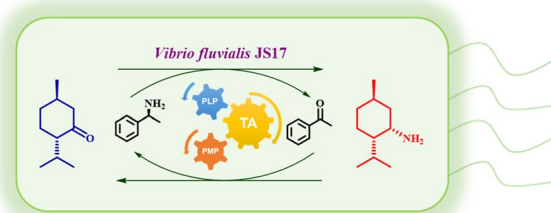
Hui-Jue Zhu¹, Jiang Pan¹, Chun-Xiu Li¹, Fei-Fei Chen^{1*} and Jian-He Xu^{1*}

Abstract

(+)-Neomenthylamine is an important industrial precursor used to synthesize high value-added chemicals. Here, we report a novel biocatalytic route to synthesize (+)-neomenthylamine by amination of readily available (–)-menthone substrate using ω -transaminase. By screening a panel of ω -transaminases, an ω -transaminase from *Vibrio fluvialis* JS17 was identified with considerable amination activity to (–)-menthone, and then characterization of enzymatic properties was conducted for the enzyme. Under optimized conditions, 10 mM (–)-menthone was transformed in a mild aqueous phase with 4.7 mM product yielded in 24 h. The biocatalytic route using inexpensive starting materials (ketone substrate and amino donor) and mild reaction conditions represents an easy and green approach for (+)-neomenthylamine synthesis. This method underscores the potential of biocatalysts in the synthesis of unnatural terpenoid amine derivatives.

Keywords Biocatalysis, (+)-Neomenthylamine, Transaminase, Asymmetric synthesis, (+)-*N*-Boc-Neomenthylamine

Graphical Abstract



*Correspondence:

Fei-Fei Chen
feifeichen@mail.ecust.edu.cn
Jian-He Xu
jianhexu@ecust.edu.cn

Full list of author information is available at the end of the article



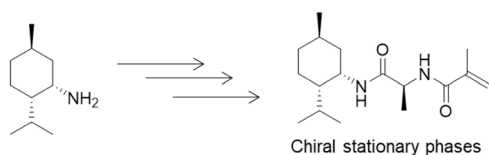
© The Author(s) 2023. **Open Access** This article is licensed under a Creative Commons Attribution 4.0 International License, which permits use, sharing, adaptation, distribution and reproduction in any medium or format, as long as you give appropriate credit to the original author(s) and the source, provide a link to the Creative Commons licence, and indicate if changes were made. The images or other third party material in this article are included in the article's Creative Commons licence, unless indicated otherwise in a credit line to the material. If material is not included in the article's Creative Commons licence and your intended use is not permitted by statutory regulation or exceeds the permitted use, you will need to obtain permission directly from the copyright holder. To view a copy of this licence, visit <http://creativecommons.org/licenses/by/4.0/>.

Introduction

Enantiomerically amines are a significant class of intermediates for the synthesis of pharmaceuticals, agrochemicals, and fine chemicals (Shin and Kim 1999; Fuchs et al. 2010; Ghislieri and Turner 2014; Costa et al. 2017). Optically pure (+)-neomenthylamine has been utilized as a building block for chiral stationary phase to resolute enantiomers in HPLC (Arlt et al. 1991). Some (+)-neomenthylamine derivatives were used as great umami flavor agents (Welschoff and Waldvogel 2010) (Scheme 1).

Currently, all the synthetic pathways of (+)-neomenthylamine rely on chemical methods with terpenoid initial reactants such as (–)-menthone (Wallach 1891; Kozlov et al. 1981; Kozlov 1982). A conventional way was to convert (–)-menthone by reductive amination under Leuckart–Wallach conditions (Kitamura et al. 2002), which could obtain all the neomenthylamines isomers. An alternative approach was to reduce menthone oxime to amines under Bouveault–Blanc conditions using an excess equivalent of sodium (Han et al. 2017). Besides, dielectrically controlled resolution (DCR) of racemic neomenthol by (*R,R*)-tartaric acid and electrochemical synthesis with mercury pool cathode were both used to produce optically pure (+)-neomenthylamine stereoselectively (Kulisch et al. 2011; Schmitt et al. 2014; Reinscheid and Reinscheid 2016). In recent reports, hydrogenation of menthone oxime to amines via gold catalysts could afford excellent yields at 100 °C. The drawbacks of this system are the high cost of gold nanoparticles and use of high temperature (Demidova et al. 2020).

Over the past 2 decades, biocatalysts are increasingly being employed for the synthesis of chiral amines due to their mild reaction conditions, high chemo/regio-selectivity, and atom economy advantages (Mayol et al. 2016; López-Iglesias et al. 2016; Wu and Li 2018; Hwang and Lee 2019; Cao et al. 2022; Wu et al. 2022). A remarkable example of industrial application is in the production process of the antidiabetic compound sitagliptin using an (*R*)-selective transaminase from *Arthrobacter* sp., which brought Merck about 6 billion U.S. dollars of revenue in 2016 (Savile et al. 2010; Ferrandi and Monti 2018).



Scheme 1 Commercial applications of (+)-neomenthylamine derivatives

In this study, we develop a simple and green biocatalytic route to synthesize (+)-neomenthylamine. The reaction is achieved by amination of (–)-menthone with a newly screened ω -transaminase from *Vibrio fluvialis* JS17 using (*S*)- α -methylbenzylamine (*S*-MBA) as amino donor in a mild aqueous phase (Scheme 2). This biocatalytic approach features apparent sustainability advantages, including avoidance of costly and poisonous catalysts, mild temperature and pressure operating conditions, easy product separation and low environmental impact, which is generally unmatched for traditional chemical methods.

Materials and methods

Materials

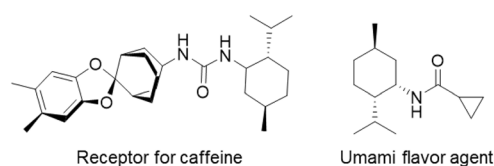
(–)-Menthone was purchased from Meryer Chemical Technology Co., Ltd. (Shanghai, China). All other reagents of analytical grade were obtained from commercial sources. Yeast extract and tryptone were purchased from Oxoid (Hampshire, UK). Genes were synthesized by Genaray Biotech Co., Ltd. (Shanghai, China). All transaminases, amine dehydrogenases, imine reductases, reductive aminases, and aminodeoxychorismate lyases were obtained from the enzyme libraries saved in our laboratory.

Gene cloning and expression

All genes were cloned into the pET-28a (+) vector and transformed into the *E. coli* BL21 (DE3) cells. Positive transformants and strains preserved in glycerol stock were grown in Luria Broth media containing 50 μ g/mL kanamycin overnight in a 37 °C incubator. Subsequently, the suspensions were transferred into Terrific Broth media for incubation until OD₆₀₀ reached to 0.6. Protein overexpression was induced by adding 0.2 mM isopropyl- β -thiogalactopyranoside (IPTG) followed by incubation for 24 h at 16 °C and 220 rpm. Cells were harvested by



Scheme 2 Synthesis of (+)-neomenthylamine via ω -transaminase VFTA-mediated amination of (–)-menthone



centrifugation at 12,000×g. All cell pellets were stored at −20 °C.

General screening

Screening reactions were carried out at 1 mL scale in Eppendorf tubes. Reaction I for the screening of amine dehydrogenases: 5 mM (−)-menthone, 1 mM NAD⁺, 1.5 mg/mL *CbFDH*, 0.2 g/mL *AmDHs* lysates in 5 M NH₄OH/NH₄COOH buffer (pH 9.0). Reaction II for the screening of transaminases and aminodeoxychorismate lyases: 5 mM (−)-menthone, 50 mM DL-Ala or isopropylamine or 2-pentanamine, 0.5 mM pyridoxal-5'-phosphate (PLP), 15 g_{cdw}/L TAs or ADCLs whole cells, 2% (v/v) DMSO in 100 mM KPb buffer (pH 8.0). Reaction III for the screening of imine reductases and reductive aminases: 5 mM (−)-menthone, 5 mM isopropylamine, 1 mM NADP⁺, 30 mM D-Glu, 3 mU/mg *BmGDH*, 0.2 g/mL IREDs or RedAms lysates in 100 mM KPb (pH 7.0). All the reactions were mixed in a high-speed shaker at 30 °C and 1000 rpm (Allsheng Instruments Co., Ltd., Hangzhou, China) and analyzed by GC–MS.

GC–MS analysis was performed on Shimadzu-QP2010 gas chromatography–mass spectrometry equipped with a Rxi[®]-5Sil MS column (30 m×0.25 mm, 0.25 μm) (injector and detector temperatures at 250 °C, oven temperature at 80 °C, ion source temperature at 230 °C, split ratio at 30:1). For analysis, the injection volume was 1 μL and the temperature of column was initially set as 80 °C, raised to 230 °C at 2 °C min^{−1} and held for 2 min.

Protein purification

Chromatography was performed on a Ni–NTA His-trap column with the following buffers: buffer A: 50 mM Tris, 500 mM NaCl, 10 mM imidazole, 0.375% (v/v) β-mercaptoethanol, pH 7.0; buffer B: 50 mM Tris, 500 mM NaCl, 500 mM imidazole, 0.375% (v/v) β-mercaptoethanol, pH 7.0; buffer C: 50 mM Tris, 150 mM NaCl, 1 mM DTT, 25% (v/v) glycerin, pH 7.0. All cells were resuspended and filtered through a 0.45-μm low protein binding membrane. The column was equilibrated with 10 column volumes of buffer A. Subsequently, enzymes were eluted with 75% buffer B after removal of non-specifically bound proteins with 25% buffer B. The purified enzymes were collected by buffer C and stored at −80 °C.

Activity assay

Enzyme activity assays of *VfTA* were performed at 30 °C for 20 min in potassium phosphate buffer (pH 6.0)

containing 5 mM (−)-menthone as substrate, 30 mM *S*-MBA as amino donor, 2 mM PLP, and 1.5 mg/mL purified enzyme. Reactions were quenched with 10 M NaOH solution, extracted with methyl tert-butyl ether (MTBE) and analyzed by GC. Kinetic parameters were determined for the amination of (−)-menthone with *VfTA*. Assay mixtures containing (0–50 mM) (−)-menthone, 60 mM *S*-MBA, 2 mM PLP, 2mg/mL purified *VfTA* in potassium phosphate buffer (pH 6.0) were incubated at 30 °C for 20 min and quenched with 10 M NaOH solution. The quenched samples were extracted with MTBE and analyzed by GC for (+)-neomenthylamine. Similar conditions were used to determine kinetic parameters for *S*-MBA with *VfTA*. All data were subjected to nonlinear regression fitting in GraphPad Prism 9.0. or Origin 2018 to obtain kinetic parameters.

GC analysis was performed on Shimadzu-2014 gas chromatography equipped with a DB-1701 column (30 m×0.25 mm, 0.25 μm) (injector temperature: 250 °C, split ratio: 30:1). For analysis, the injection volume was 1 μL and the temperature of column was initially set as 50 °C, raised to 90 °C at 10 °C min^{−1}, and then increased to 260 °C at 20 °C min^{−1}.

Thermostability assay

Half-life and melting temperature (T_m) assays of *VfTA* were determined in this study. The purified *VfTA* was diluted to 2 mg/mL with buffer C and incubated at 30 °C, 40 °C, and 50 °C, respectively. Samples were extracted at regular intervals to calculate residual activity through GC analysis.

Data were subjected to first-order inactivation kinetic equation for nonlinear regression fitting to obtain $t_{1/2}$ in Origin 2018. T_m assays of *VfTA* were determined by detecting the CD absorbance values in the wavelength range of 180–260 nm at various temperatures using a circular dichroism spectrometer (Applied Photophysics Ltd., Oxford, UK). Data were analyzed with Global 3 analysis to determine T_m values.

Bioinformatics

MEGA 11 was used to perform multiple sequence alignment. Phylogenetic trees were built with the neighbor-joining algorithm within the Molecular Evolutionary Genetics Analysis Version 11 (MEGA 11) and present the relative positions of the proteins labeled with species name (Lewis et al. 1995). Molecular modeling for this project was performed using crystal structures of *Vibrio fluvialis* JS17 (PDB:5ZTX) and various ligands were docked by AutoDock Vina program package. The center grid box was defined by x, y, z coordinates of −1.437, −5.754, and 20.424, respectively, with a volume size of 15*15*15.

Scale-up protocol

A preparative-scale mixture with a volume of 300 mL, containing 10 mM (–)-menthone, 60 mM *S*-MBA, 2 mM PLP, and 100 g/L *VfTA* whole cells in potassium phosphate buffer (pH 6.0) was incubated at 30 °C and 200 rpm for 28 h. The reaction was stopped by adding 15 mL 10 M NaOH solution and extracted with MTBE (3×300 mL). The organic extract was dried over anhydrous Na₂SO₄ and concentrated under reduced pressure vacuum to obtain (+)-neomenthylamine product.

Boc derivatization

Mixture of 5 mmol (+)-neomenthylamine, 7.5 mmol di-tert-butyl-dicarbonate, and 5 mmol TEA was dissolved in 500 mL DCM. The reaction was maintained at room temperature with reflux using a condenser for 4 h. Reaction mixture after concentration was separated on silica gel column with PE/EA=200/1 (v/v). The organic phase was concentrated under reduced pressure to obtain (+)-Boc-neomenthylamine product.

Results and discussion

Discovery of an ω-transaminase for amination of (–)-menthone to (+)-neomenthylamine

Since the enzymatic reaction pathway from (–)-menthone to (+)-neomenthylamine has not been reported yet, we dissected the chemical structure of (–)-menthone and observed that it features a cyclohexane skeleton with a carbonyl group and alkyl substitutions. Leveraging this characteristic, we devised a substrate analog screening strategy, employing the amination of cyclohexanone or its analogs as a model reaction to discover enzymes that can convert (–)-menthone to (+)-neomenthylamine.

Subsequently, we screened 83 target enzymes from different sources capable of catalyzing amination reaction, including transaminases (TAs), imine reductases (IREDs), reductive amine enzymes (RedAms), amine dehydrogenases (AmDHs), and aminodeoxychorismate lyases (ADCLs) (Koszelewski et al. 2011; Tufvesson et al. 2012; Skalden et al. 2015; Wetzl et al. 2016; Guo and Berglund 2017; Ramsden et al. 2019; Gavin et al. 2019; Mangas-Sanchez et al. 2020). After expressing and rescreening of the enzymes in the form of cell-free extract, we obtained a transaminase (*VfTA*) from *Vibrio fluvialis* JS17 (PDB: 5ZTX) that can convert (–)-menthone into (+)-neomenthylamine successfully. A phylogenetic analysis was constructed to analyze the evolutionary relationship of *VfTA* with the previously reported ω-transaminases that catalyze the amination of cyclohexanone and its analogs (Fig. 1). As a result, *VfTA* was situated at the same clade with the transaminases from *Pseudovibrio* sp. WM33 and *Chromobacterium violaceum* ATCC 12472, demonstrating a relatively close evolutionary relationship with the two enzymes.

Different amino donors were then investigated for *VfTA*-catalyzed amination of menthone, and interestingly, *VfTA* exhibited different activities and selectivities for different amino donors (Table 1). Compared with DL-alanine and 2-pentanamine, using isopropylamine as the amino donor resulted in the highest yield of (+)-neomenthylamine by *VfTA*, reaching 0.19 mM with a conversion rate of 3.8%.

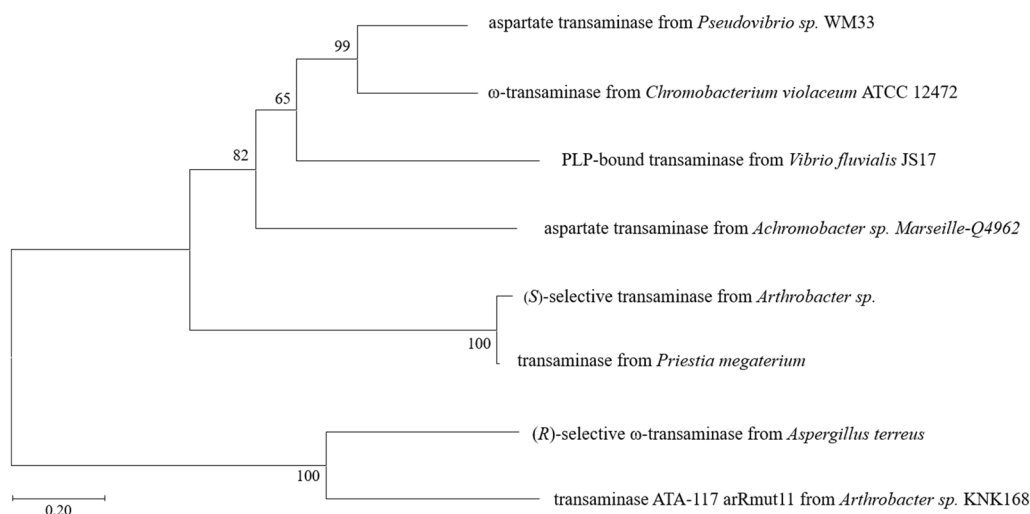


Fig. 1 Phylogenetic analysis of the *VfTA* and the homologous proteins

Table 1 Asymmetric synthesis of (+)-neomenthylamine using *VfTA* with different amino donors

Enzyme	DL-Ala		Isopropylamine		2-Pentanamine	
	Conv. (%) ^a	d.e. (%) ^b	Conv. (%) ^a	d.e. (%) ^b	Conv. (%) ^a	d.e. (%) ^b
<i>VfTA</i>	0.9	79 (3 <i>S</i> , 4 <i>S</i>)	3.8	82 (3 <i>S</i> , 4 <i>S</i>)	2.1	80 (3 <i>S</i> , 4 <i>S</i>)

^a Conversion and the value of diastereomeric excess was determined by GC–MS on an achiral phase. The screening reaction system (1 mL) consists of potassium salt phosphate buffer (100 mM KPB pH 8.0), 5 mM (–)-menthone, 50 mM DL-Ala or isopropylamine or 2-pentanamine, 0.5 mM pyridoxal-5′-phosphate (PLP), 15 g_{cdw} L⁻¹ whole cells, 10% (v/v) dimethyl sulfoxide. All the reaction mixtures were shaken for 24 h at 30 °C and 1000 rpm in a high-speed shaker

^b D.e. (%) = $\frac{|[(3*S*,4*S*)+(3*R*,4*S*)]-[(3*S*,*R*)+(3*R*,4*R*)]|}{[(3*S*,4*S*)+(3*R*,4*S*)]+[(3*S*,4*R*)+(3*R*,4*R*)]}$

Optimization of system parameters for *VfTA*-mediated transamination reaction

To improve the efficiency of *VfTA*-mediated reaction for (+)-neomenthylamine production, the effects of some reaction parameters were investigated, including amino donor types and equivalents, pH, temperature, and PLP dose. For transaminases, unfavorable thermodynamic equilibrium is an important bottleneck limiting the reaction (Slabu et al. 2018), and adding excessive amino donor usually can help to overcome this defect. We selected nine commonly used amino donors with different carbon chain lengths and steric hindrance sizes. Among them, *S*-MBA as an amino donor exhibited excellent catalytic efficiency for the transaminase reaction (Fig. 2).

The optimal pH and temperature for the reaction were determined to be pH 6.0 (Fig. 3A) and 30 °C (Fig. 3B), respectively. The titer of (+)-neomenthylamine raised with the increase of amino donor equivalent, and the highest titer of (+)-neomenthylamine was observed when 60 mM of *S*-MBA was loaded (Fig. 3C). However, further increase of amino donor equivalent posed a detrimental effect on the yield of (+)-neomenthylamine (Ge et al. 2022). Besides, the dosage of cofactor PLP (pyridoxal-5′-phosphate) was also optimized, indicating that 2 mM PLP was sufficient for the single-step reaction (Fig. 3D).

Kinetic analysis for *VfTA* showed potential co-substrate and co-product inhibition

VfTA from *V. fluvialis* JS17 belongs to the class III transaminases of the fold type I PLP family, which follows a ping-pong bi-bi reaction mechanism (Slabu et al. 2017). Amino donor *S*-MBA participates in the reaction as a co-substrate. Wild-type *VfTA* was purified and used for determination of kinetic constants (Table 2). As a result, *VfTA* had very limited catalytic efficiency (k_{cat}/K_M) for the substrate (–)-menthone, whereas it had remarkable higher catalytic efficiency (k_{cat}/K_M) for amino donor *S*-MBA.

In the structure of *VfTA* (PDB: 5ZTX), cofactor PLP was covalently linked to lysine 285 through Schiff base, forming a highly conserved catalytic domain. This linkage affected the conformational stability and flexibility of the dimer interface, including the catalytic region

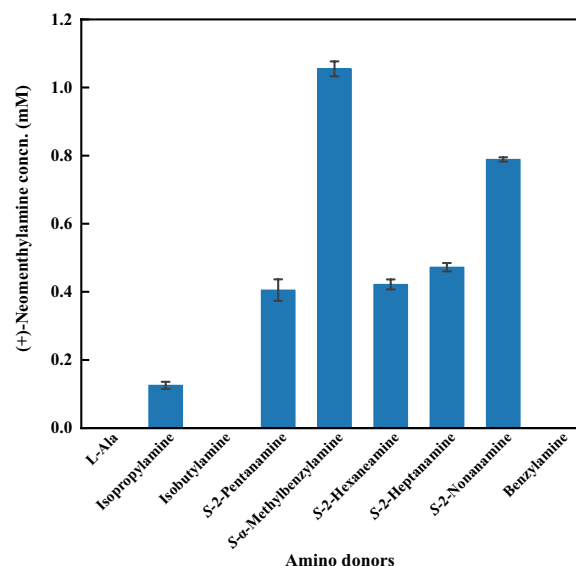


Fig. 2 Effect of amino donors of *VfTA* on the production of (+)-neomenthylamine. Reaction conditions (1 mL): 5 mM (–)-menthone, 2 mg/mL purified *VfTA*, 1 mM PLP, KPB buffer (100 mM pH 7.0), 1% DMSO, in addition to 50 mM amino donor of L-Ala, isopropylamine, isobutylamine, (*S*)-2-pentanamine, (*S*)-2-hexanamine, (*S*)-2-heptanamine, (*S*)-2-nonanamine, (*S*)-α-methylbenzylamine or benzylamine. All mixtures were shaken at 30 °C, 1000 rpm for 24 h.

(Additional file 1: Fig. S1). Next, we established molecular models between crystal structure and different ligands through AutoDock Vina. The docking analysis showed that the ligand *S*-MBA adopted a flat conformation within the binding pocket, while (–)-menthone faced more steric hindrance due to its inherent chair structure (Additional file 1: Fig. S2). Meanwhile, protein–ligand interaction analysis revealed that *S*-MBA had more hydrophobic interactions and hydrogen bonds with surrounding residues compared with (–)-menthone, promoting its binding to the enzyme. The π–π stacking interaction between *S*-MBA and Y150 stabilized the binding of the amino donor, playing a crucial role in activating activity (Additional file 1: Fig. S3). Notably, this situation was in accordance with the significantly lower K_M value of *VfTA* for *S*-MBA

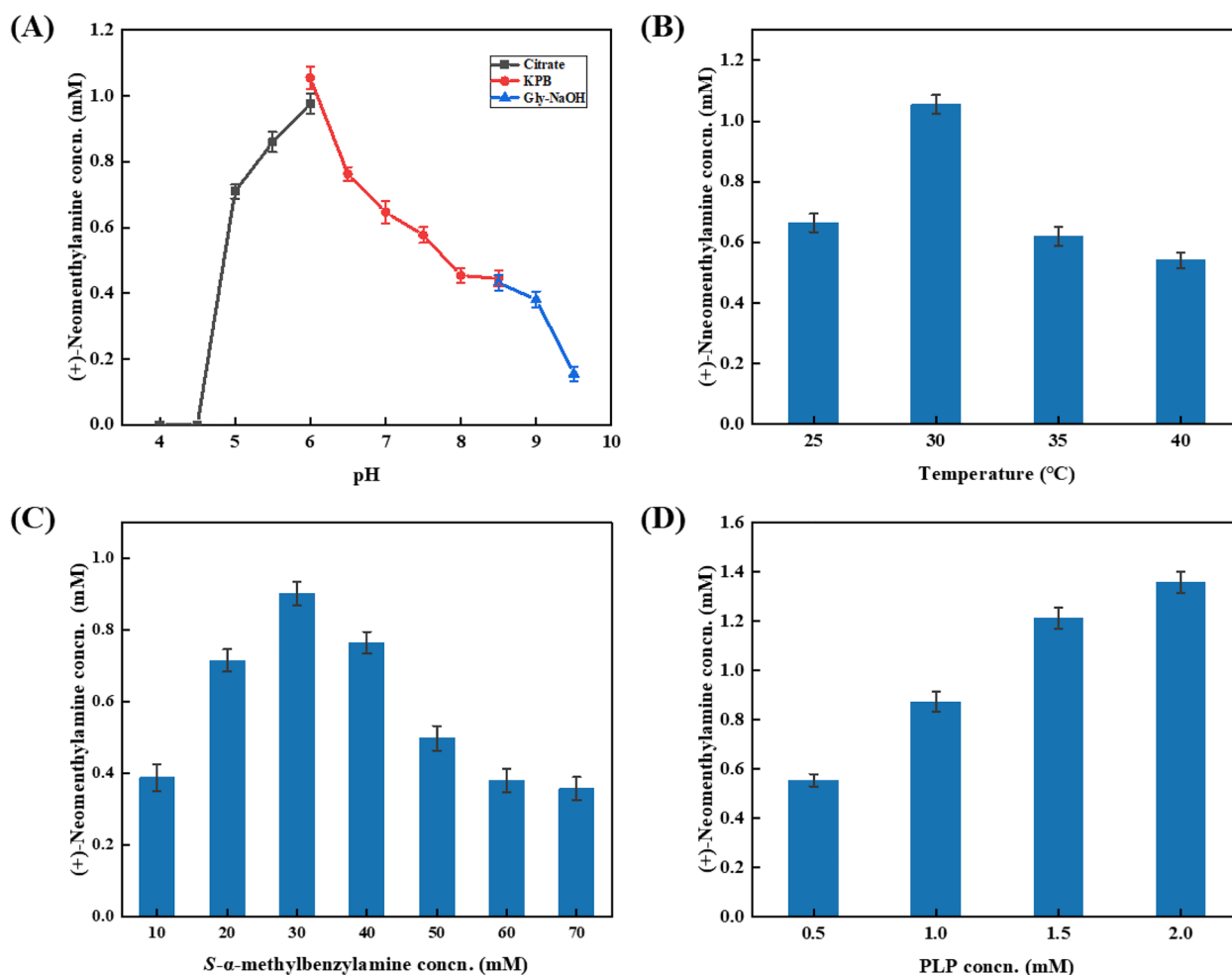


Fig. 3 Optimization of the system parameters of *VfTA*-catalyzed transamination. Reaction conditions (1 mL): 5 mM (–)-menthone, 50 mM (*S*-α-methylbenzylamine, 2 mg/mL purified *VfTA*, 1 mM PLP, KPB buffer (100 mM pH 7.0), 1% DMSO, 30 °C, 1000 rpm for 24 h, unless otherwise noted. **(A)** citrate buffer (100 mM pH 4.0–6.0) or potassium phosphate buffer (100 mM pH 6.0–8.5) or Gly-NaOH buffer (100 mM pH 8.5–9.5); **(B)** incubation temperature: 25 °C, 30 °C, 35 °C, or 40 °C; **(C)** 10–70 mM (*S*-α-methylbenzylamine); **(D)** 0.5–2 mM PLP.

Table 2 Kinetic constants of *VfTA* toward substrate (–)-menthone and amino donor *S*-MBA^a

Entry	Compound	V_{max} (U/mg)	K_M (mM)	k_{cat} (s^{-1})	k_{cat}/K_M ($s^{-1}mM^{-1}$)
<i>VfTA</i>	(–)-Menthone	0.0054±0.0002	5.0±0.6	16.3±0.0	3.3
	(<i>S</i>)-α-Methyl benzylamine	0.014±0.000	0.8±0.1	42.3±0.0	54.4

^a All reactions were carried out in triplicates, and the average values with standard deviation were shown. The kinetic curves of *VfTA* for substrate and amino donor were fitted by Prism 9

compared to (–)-menthone, indicating a stronger affinity of *VfTA* toward *S*-MBA.

We also investigated whether the amination of (–)-menthone by *VfTA* was affected by substrate or product inhibition during the reaction. Using the inhibition

model established based on Michaelis–Menten equation (Choi et al. 2017), the corresponding inhibition constants were calculated (Table 2). Unusually, *VfTA* exhibited substrate inhibition and product inhibition for *S*-MBA and acetophenone, while no corresponding inhibitions were detected for (–)-menthone and (+)-neomenthylamine. Furthermore, *VfTA* had a much lower K_i value for acetophenone compared with *S*-MBA, resulting in a ninefold difference in K_i . Even when 20 mM acetophenone was added, the rate of enzymatic reaction was almost undetectable (Table 3).

Thermostability analysis of *VfTA*

The thermostability of *VfTA* was explored by both melting temperature (T_m) measurements and half-life ($t_{1/2}$) measurements after incubation at different temperatures.

Table 3 Inhibition constants of *VfTA* toward *S*-MBA and acetophenone

Entry	Compound	K_i (mM)
<i>VfTA</i>	<i>S</i> - α -Methylbenzylamine	5.8 ± 0.7
	Acetophenone	0.6 ± 0.0

^a All reactions were carried out in triplicates, and the average values with standard deviation were shown. The kinetic curves of *VfTA* for *S*-MBA and acetophenone were fitted by Origin 2018

The T_m value of *VfTA* (0.5 mg/mL) in KPB buffer (100 mM, pH 6.0) was determined to be 65.6 °C (Additional file 1: Fig. S4). The deactivation rate constant (k_d) and $t_{1/2}$ following the first-order enzymatic inactivation kinetic equation were also determined. As shown in Table 4 and Additional file 1: Fig. S4, the $t_{1/2}$ of *VfTA* at 30 °C was close to 2 days, and even at 50 °C, it could still be maintained for 3 h. Thus, it is evident that *VfTA* possesses commendable thermal stability.

300 mL preparative-scale bioreaction

Finally, we performed a 300 mL preparative-scale bioreaction under optimal conditions, where the time-course analysis revealed that the yield of (+)-neomenthylamine reached a maximum 4.7 mM at 24 h approximately (Fig. 4). Surprisingly, we observed that (–)-menthone undergoes racemization in aqueous solution at the beginning of the reaction, generating a small portion of (+)-isomenthone. Subsequently, (+)-isomenthone was transaminated to produce (+)-isomenthylamine, and the side reaction reached equilibrium after 12 h. The reaction was incubated for 28 h, and after derivatization and purification, 150 mg of *N*-Boc derivatized (+)-neomenthylamine product was obtained with 33% yield. $[\alpha]_D^{23} = +30$ (c 1.7, ethyl acetate). $^1\text{H NMR}$ (600 MHz, CDCl_3): δ 4.52 (d, $J=8.5$ Hz, 1H), 4.00–3.91 (m, 1H), 1.77 (d, $J=13.3$ Hz, 1H), 1.74–1.68 (m, 1H), 1.68–1.58 (m, 2H), 1.37 (s, 9H), 1.34–1.28 (m, 1H), 1.00–0.87 (m, 3H), 0.85 (d, $J=6.7$ Hz, 3H), 0.82 (d, $J=6.6$ Hz, 3H), 0.80 (d, $J=6.5$ Hz, 3H), 0.78–0.75 (m, 1H).

Thus, the pathway for synthesizing (+)-neomenthylamine using biocatalyst has been well established, where mild aqueous conditions are used, all the reactants used in this route [(–)-menthone, *S*-MBA, and PLP] are

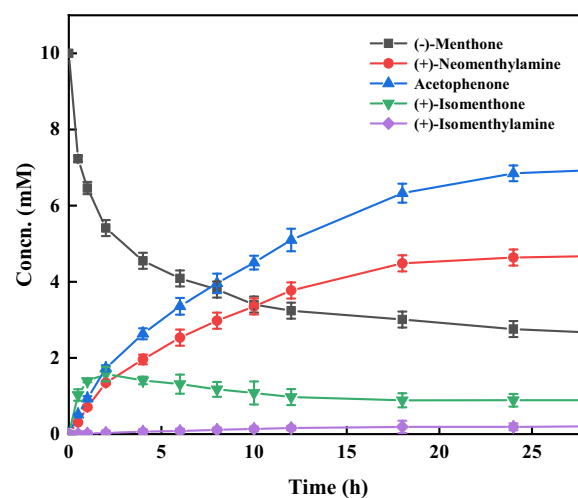


Fig. 4 Time courses of the 300 mL preparative-scale asymmetric synthesis of (+)-neomenthylamine. Reaction condition: 10 mM (–)-menthone, 60 mM *S*-MBA, 100 g L⁻¹ *VfTA* whole cells, 2 mM PLP, KPB (100 mM pH 6.0), 30 °C and 200 rpm, 28 h

inexpensive, and the process generated the easily removable by-product acetophenone, with minor environmental impact. In contrast to the previously reported chemical methods, the constructed biocatalytic approach could represent an easier and greener approach for (+)-neomenthylamine synthesis. A number of strategies that may be utilized to further enhance the yield, such as continuous feeding of amino donors, or in situ removal of co-products. In addition, a significant advantage of *VfTA* is its excellent stability. Freeze-dried *VfTA* enzyme powder is readily available and could maintain its catalytic activity for decades when stored at 4 °C.

Conclusion

In summary, we developed a novel and simple route to achieve the biosynthesis of (+)-neomenthylamine. By screening a number of wild-type enzymes, an ω -transaminase *VfTA* from *Vibrio fluvialis* JS17 capable of synthesizing (+)-neomenthylamine was obtained. After systematic characterization of enzymatic properties and kinetics analysis, a 300 mL scaled-up bioreaction was conducted with considerable yield. In contrast to the previously reported chemical methods, the constructed biocatalytic approach avoided the use

Table 4 Determination of thermostability parameters of *VfTA*

Entry	30 °C		40 °C		50 °C		T_m^a °C
	k_d /h	$t_{1/2}$ /h	k_d /h	$t_{1/2}$ /h	k_d /h	$t_{1/2}$ /h	
<i>VfTA</i>	0.02	44.1	0.09	8.1	0.2	3.1	65.6 ± 0.4

^a The melting temperature (T_m) curves of *VfTA* were fitted by Global 3 T-Ramp

of expensive and poisonous catalysts, harsh operation conditions, and generation of excess wastes, thus representing an easy and green approach for (+)-neomenthylamine synthesis. More works of protein engineering and process optimization may be necessary to further improve the efficiency of biotransformation and to minimize the waste of the excessive co-substrate. The refined enzymatic route might provide new accesses to other structurally varied terpene-derived primary amines and associated optically active compounds.

Abbreviations

S-MBA	S- α -Methylbenzylamine
KPB	Potassium phosphate buffer
DMSO	Dimethyl sulfoxide
D.e.	Diastereomeric excess
Concn.	Concentration
VfTA	Transaminase from <i>Vibrio fluvialis</i> JS17
CbFDH	Formate dehydrogenase from <i>Candida boidinii</i>
BmGDH	Glucose dehydrogenase from <i>Bacillus megaterium</i>
NADH	Nicotinamide adenine dinucleotide
NADPH	Nicotinamide adenine dinucleotide phosphate
PLP	Pyridoxal-5'-phosphate
TAs	Transaminases
IREDs	Imine reductases
AmDHs	Amine dehydrogenases
RedAms	Reductive aminases
ADCLs	Aminodeoxychorismate lyases

Supplementary Information

The online version contains supplementary material available at <https://doi.org/10.1186/s40643-023-00693-w>.

Additional file 1: Table S1. Amino acids sequences of enzymes for functional screening. **Figure S1.** Dimeric structure of ω -transaminase from *Vibrio fuvialis* JS17. **Figure S2.** Docking results of different ligands with VfTA. **Figure S3.** Interactions between different ligands and residues. **Figure S4.** Melting temperatures of the VfTA. **Figure S5.** Kinetic curves of inhibition of VfTA towards S-MBA and acetophenone. **Figure S6.** Kinetic curves of VfTA towards substrate and amino donor. **Figure S7.** ^1H NMR and ^{13}C NMR spectra of the (+)-*N*-Boc-neomenthylamine.

Acknowledgements

We thank the research and development platform provided by State Key Laboratory of Bioreactor Engineering, Shanghai Collaborative Innovation Centre for Biomanufacturing, Frontiers Science Center for Materiobiology and Dynamic Chemistry, East China University of Science and Technology.

Author contributions

HJZ: methodology, investigation, data curation, visualization, writing original draft. FFC: methodology, funding acquisition, reviewing and editing manuscript. JHX: supervision, funding acquisition, project administration, reviewing and editing manuscript. All authors read and approved the final manuscript.

Funding

This work was financially supported by the National Key Research and Development Program of China (2019YFA0905000 and 2021YFA0911400) and the National Natural Science Foundation of China (21871085 and 31971380), and the Fundamental Research Funds for the Central Universities (222201714026).

Availability of data and materials

All data generated or analyzed during this study are included in this article and its supplementary information file.

Declarations

Ethics approval and consent to participate

Not applicable.

Consent for publication

Not applicable.

Competing interests

The first authors declare that the corresponding author is the editor-in-chief of the journal.

Author details

¹Laboratory of Biocatalysis and Synthetic Biotechnology, State Key Laboratory of Bioreactor Engineering, Shanghai Collaborative Innovation Centre for Biomanufacturing, College of Biotechnology, East China University of Science and Technology, Shanghai 200237, People's Republic of China.

Received: 9 June 2023 Accepted: 9 October 2023

Published online: 03 November 2023

References

- Arlt D, Bömer B, Grosser R, Lange W (1991) New chiral polyamide stationary phases for chromatographic enantiomer separation. *Angew Chem Int Ed Engl* 30:1662–1664. <https://doi.org/10.1002/anie.199116621>
- Cao W, Li H, Chen F et al (2022) Modification and characterization of imine reductases for synthesis of 1-Phenyl-1,2,3,4-Tetrahydro-Isoquinoline. *J East China Univ Sci Technol* 48:511–518. <https://doi.org/10.14135/j.cnki.1006-3080.20210505001>
- Choi B, Rempala GA, Kim JK (2017) Beyond the Michaelis-Menten equation: accurate and efficient estimation of enzyme kinetic parameters. *Sci Rep* 7:17018. <https://doi.org/10.1038/s41598-017-17072-z>
- Costa ICR, de Souza ROMA, Bornscheuer UT (2017) Asymmetric synthesis of serinol-monoesters catalyzed by amine transaminases. *Tetrahedron Asymmetry* 28:1183–1187. <https://doi.org/10.1016/j.tetasy.2017.08.012>
- Demidova YuS, Mozhaitsev ES, Suslov EV et al (2020) Menthylamine synthesis via gold-catalyzed hydrogenation of menthone oxime. *Appl Catal A* 605:117799. <https://doi.org/10.1016/j.apcata.2020.117799>
- Ferrandi EE, Monti D (2018) Amine transaminases in chiral amines synthesis: recent advances and challenges. *World J Microbiol Biotechnol* 34:13. <https://doi.org/10.1007/s11274-017-2395-2>
- Fuchs M, Koszelewski D, Tauber K et al (2010) Chemoenzymatic asymmetric total synthesis of (S)-Rivastigmine using ω -transaminases. *Chem Commun* 46:5500. <https://doi.org/10.1039/c0cc00585a>
- Gavin DP, Reen FJ, Rocha-Martin J et al (2019) Genome mining and characterisation of a novel transaminase with remote stereoselectivity. *Sci Rep* 9:20285. <https://doi.org/10.1038/s41598-019-56612-7>
- Ge Y, Huang Z-Y, Pan J et al (2022) Regiospecific C-H amination of (–)-limonene into (–)-perillamine by multi-enzymatic cascade reactions. *Bioresour Bioprocess* 9:88. <https://doi.org/10.1186/s40643-022-00571-x>
- Ghislieri D, Turner NJ (2014) Biocatalytic approaches to the synthesis of enantiomerically pure chiral amines. *Top Catal* 57:284–300. <https://doi.org/10.1007/s11244-013-0184-1>
- Guo F, Berglund P (2017) Transaminase biocatalysis: optimization and application. *Green Chem* 19:333–360. <https://doi.org/10.1039/C6GC02328B>
- Han M, Ma X, Yao S et al (2017) Development of a modified Bouveault-Blanc reduction for the selective synthesis of α , α -dideuterio alcohols. *J Org Chem* 82:1285–1290. <https://doi.org/10.1021/acs.joc.6b02950>
- Hwang ET, Lee S (2019) Multienzymatic cascade reactions via enzyme complex by immobilization. *ACS Catal* 9:4402–4425. <https://doi.org/10.1021/acscatal.8b04921>
- Kitamura M, Lee D, Hayashi S et al (2002) Catalytic Leuckart–Wallach-type reductive amination of ketones. *J Org Chem* 67:8685–8687. <https://doi.org/10.1021/jo0203701>
- Koszelewski D, Grischek B, Glueck SM et al (2011) Enzymatic racemization of amines catalyzed by enantiocomplementary ω -transaminases. *Chem Eur J* 17:378–383. <https://doi.org/10.1002/chem.201001602>

- Kozlov NG (1982) Advances in the field of the synthesis of amino derivatives of terpenoids. *Chem Nat Compd* 18:131–143. <https://doi.org/10.1007/BF00577177>
- Kozlov NG, Pekhk TI, Vyalimyaé TK (1981) Reductive amination of menthol by aliphatic nitriles. *Chem Nat Compd* 17:238–243. <https://doi.org/10.1007/BF00568510>
- Kulisch J, Nieger M, Stecker F et al (2011) Efficient and stereodivergent electrochemical synthesis of optically pure menthylamines. *Angew Chem Int Ed* 50:5564–5567. <https://doi.org/10.1002/anie.201101330>
- Lewis PO, Kumar S, Tamura K, Nei M (1995) MEGA: molecular evolutionary genetics analysis, Version 1.02. *Syst Biol* 44:576. <https://doi.org/10.2307/2413665>
- López-Iglesias M, González-Martínez D, Gotor V et al (2016) Biocatalytic transamination for the asymmetric synthesis of pyridylalkylamines. Structural and activity features in the reactivity of transaminases. *ACS Catal* 6:4003–4009. <https://doi.org/10.1021/acscatal.6b00686>
- Mangas-Sanchez J, Sharma M, Cosgrove SC et al (2020) Asymmetric synthesis of primary amines catalyzed by thermotolerant fungal reductive aminases. *Chem Sci* 11:5052–5057. <https://doi.org/10.1039/D0SC02253E>
- Mayol O, David S, Darii E et al (2016) Asymmetric reductive amination by a wild-type amine dehydrogenase from the thermophilic bacteria *Petrogoga mobilis*. *Catal Sci Technol* 6:7421–7428. <https://doi.org/10.1039/C6CY01625A>
- Ramsden JI, Heath RS, Derrington SR et al (2019) Biocatalytic N-alkylation of amines using either primary alcohols or carboxylic acids via reductive aminase cascades. *J Am Chem Soc* 141:1201–1206. <https://doi.org/10.1021/jacs.8b11561>
- Reinscheid F, Reinscheid UM (2016) Stereochemical analysis of menthol and menthylamine isomers using calculated and experimental optical rotation data. *J Mol Struct* 1103:166–176. <https://doi.org/10.1016/j.molstruc.2015.09.013>
- Savile CK, Janey JM, Mundorff EC et al (2010) Biocatalytic asymmetric synthesis of chiral amines from ketones applied to sitagliptin manufacture. *Science* 329:305–309. <https://doi.org/10.1126/science.1188934>
- Schmitt M, Schollmeyer D, Waldvogel SR (2014) Efficient resolution of menthylamine with inexpensive (*R,R*)-tartaric acid by dielectrically controlled resolution (DCR): efficient resolution of menthylamine. *Eur J Org Chem* 2014:1007–1012. <https://doi.org/10.1002/ejoc.201301566>
- Shin J-S, Kim B-G (1999) Asymmetric synthesis of chiral amines with ω -transaminase. *Biotechnol Bioeng* 65:206–211. [https://doi.org/10.1002/\(SICI\)1097-0290\(19991020\)65:2%3C206::AID-BIT11%3E3.0.CO;2-9](https://doi.org/10.1002/(SICI)1097-0290(19991020)65:2%3C206::AID-BIT11%3E3.0.CO;2-9)
- Skalden L, Peters C, Dickerhoff J et al (2015) Two subtle amino acid changes in a transaminase substantially enhance or invert enantiopreference in cascade syntheses. *ChemBioChem* 16:1041–1045. <https://doi.org/10.1002/cbic.201500074>
- Slabu I, Galman JL, Lloyd RC, Turner NJ (2017) Discovery, engineering, and synthetic application of transaminase biocatalysts. *ACS Catal* 7:8263–8284. <https://doi.org/10.1021/acscatal.7b02686>
- Slabu I, Galman JL, Iglesias C et al (2018) *n*-Butylamine as an alternative amine donor for the stereoselective biocatalytic transamination of ketones. *Catal Today* 306:96–101. <https://doi.org/10.1016/j.cattod.2017.01.025>
- Tufvesson P, Jensen JS, Kroutil W, Woodley JM (2012) Experimental determination of thermodynamic equilibrium in biocatalytic transamination. *Biotechnol Bioeng* 109:2159–2162. <https://doi.org/10.1002/bit.24472>
- Wallach O (1891) Ueber Menthylamin. *Ber Dtsch Chem Ges* 24:3992–3993. <https://doi.org/10.1002/cber.189102402292>
- Welschoff N, Waldvogel S (2010) Practical synthesis of optically pure menthylamines starting from racemic neomenthol. *Synthesis* 2010:3596–3601. <https://doi.org/10.1055/s-0030-1258295>
- Wetzel D, Gand M, Ross A et al (2016) Asymmetric reductive amination of ketones catalyzed by imine reductases. *ChemCatChem* 8:2023–2026. <https://doi.org/10.1002/cctc.201600384>
- Wu S, Li Z (2018) Whole-cell cascade biotransformations for one-pot multistep organic synthesis. *ChemCatChem* 10:2164–2178. <https://doi.org/10.1002/cctc.201701669>
- Wu Q-Y, Huang Z-Y, Wang J-Y et al (2022) Construction of an *Escherichia coli* cell factory to synthesize taxadien-5 α -ol, the key precursor of anti-cancer drug paclitaxel. *Bioresour Bioprocess* 9:82. <https://doi.org/10.1186/s40643-022-00569-5>

Publisher's Note

Springer Nature remains neutral with regard to jurisdictional claims in published maps and institutional affiliations.

Submit your manuscript to a SpringerOpen® journal and benefit from:

- Convenient online submission
- Rigorous peer review
- Open access: articles freely available online
- High visibility within the field
- Retaining the copyright to your article

Submit your next manuscript at ► [springeropen.com](https://www.springeropen.com)